The Human Cytomegalovirus Transmembrane Protein pUL50 Induces Loss of VCP/p97 and Is Regulated by a Small Isoform of pUL50

Myoung Kyu Lee,[a] Seokhwan Hyeon,[a] (ID) Jin-Hyun Ahn[a,b]

[a]Department of Microbiology, Sungkyunkwan University School of Medicine, Suwon, Republic of Korea
[b]Samsung Biomedical Research Institute, Samsung Medical Center, Seoul, Republic of Korea

ABSTRACT The human cytomegalovirus (HCMV) UL50 gene encodes a transmembrane protein, pUL50, which acts as a core component of the nuclear egress complex (NEC) for nucleocapsids. Recently, pUL50 has been shown to have NEC-independent activities: downregulation of IRE1 to repress the unfolded protein response and degradation of UBE1L to inhibit the protein ISG15 modification pathway. Here, we demonstrate that a 26-kDa N-terminal truncated isoform of pUL50 (UL50-p26) is expressed from an internal methionine at amino acid position 199 and regulates the activity of pUL50 to induce the loss of valosin-containing protein (VCP/p97). A UL50(M199V) mutant virus expressing pUL50(M199V) but not UL50-p26 showed delayed growth at a low multiplicity of infection. There was also delayed accumulation of the viral immediate early 2 (IE2) protein in the mutant virus, and this correlated with the reduced expression of VCP/p97, which promotes IE2 expression. Infection with mutant virus did not significantly alter ISGylation levels. In transient expression assays, pUL50 induced VCP/p97 loss posttranscriptionally, and this was dependent on the presence of its transmembrane domain. In contrast, UL50-p26 did not destabilize VCP/p97 but, rather, inhibited pUL50-mediated VCP/p97 loss and the associated major IE gene suppression. Both pUL50 and UL50-p26 interacted with VCP/p97, although UL50-p26 did so more weakly than pUL50. UL50-p26 interacted with pUL50, and this interaction was much stronger than the pUL50 self-interaction. Furthermore, UL50-p26 was able to interfere with the pUL50-VCP/p97 interaction. Our study newly identifies UL50-p26 expression during HCMV infection and suggests a regulatory role for UL50-p26 in blocking pUL50-mediated VCP/p97 loss by associating with pUL50.

IMPORTANCE Targeting the endoplasmic reticulum (ER) by viral proteins may affect ER-associated protein homeostasis. During human cytomegalovirus (HCMV) infection, pUL50 targets the ER through its transmembrane domain and moves to the inner nuclear membrane (INM) to form the nuclear egress complex (NEC), which facilitates capsid transport from the nucleus to the cytoplasm. Here, we demonstrate that pUL50 induces the loss of valosin-containing protein (VCP/p97), which promotes the expression of viral major immediate early gene products, in a manner dependent on its membrane targeting but that a small isoform of pUL50 is expressed to negatively regulate this pUL50 activity. This study reports a new NEC-independent function of pUL50 and highlights the fine regulation of pUL50 activity by a smaller isoform for efficient viral growth.

KEYWORDS human cytomegalovirus, UL50, VCP/p97

Herpesviruses have a large double-stranded DNA genome. During viral replication, the nucleocapsid is assembled in the nucleus and moves to the cytoplasm across the nuclear membrane. The nuclear egress of capsids requires the formation of the

nuclear egress complex (NEC) (for reviews, see references 1 to 5). Herpesviruses encode two core components of the NEC. In human cytomegalovirus (HCMV), which belongs to the betaherpesvirus subfamily, these core components are pUL50 and pUL53, which interact with each other (6, 7). These proteins are conserved in other herpesviruses. pUL34 of herpes simplex virus 1 (HSV-1), BFRF1 of Epstein-Barr virus (EBV), and ORF67 of Kaposi's sarcoma-associated herpesvirus (KSHV) are functional homologs of pUL50 of HCMV. The NEC function of pUL53 of HCMV is also conserved in pUL31 of HSV-1, BFLF2 of EBV, and ORF69 of KSHV (8–11).

The formation of the NEC is a complicated process. In HCMV, pUL50 initially targets the endoplasmic reticulum (ER) through its transmembrane (TM) domain and reaches the inner nuclear membrane (INM) during the late stages of infection, where it associates with phosphoprotein pUL53, which enters through the nuclear pore using a nuclear localization signal (NLS), resulting in formation of the core NEC. Once the core NEC is formed, other NEC components, such as p32/gC1qR, emerin, viral protein kinase pUL97, cellular protein kinase C isoform a (PKCa), and cellular cyclin-dependent kinase 1 (CDK1), are recruited to the nuclear rim, forming the functional NEC (6, 12–15).

It has recently been reported that pUL50 may have other activities that are independent of NEC function. Inositol-requiring enzyme 1 (IRE1) mediates mRNA splicing of the X-box binding protein 1 (XBP1) in the unfolded protein response (UPR). The M50 protein of mouse cytomegalovirus (MCMV), a homolog of pUL50 of HCMV, has been shown to interact with IRE1 and downregulate its expression during viral infection. In transfection assays, the expression of M50 was sufficient for IRE1 downregulation, and this activity required its transmembrane domain. Similar activity was observed for pUL50 of HCMV (16). We also found that pUL50 inhibits protein modification by ISG15 (ISGylation) by inducing proteasomal degradation of UBE1L, an E1-activating enzyme for ISGylation. This activity of pUL50 also requires its transmembrane domain within the C-terminal region. Furthermore, pUL50 interacts with RNF170, an ER-associated E3 ligase, and this interaction promotes pUL50-mediated UBE1L degradation via ubiquitination (17). These observations suggest that pUL50 and its homologs may regulate membrane-associated cellular activities when they target the ER.

In this study, we identified that a smaller 26-kDa isoform of pUL50, referred to here as UL50-p26, is expressed using an internal methionine codon of the UL50 gene during HCMV infection. During investigation of the role of UL50-p26 in viral infection, we discovered that pUL50 has activity to posttranscriptionally downregulate the expression of valosin-containing protein (VCP/p97), which has been shown to promote HCMV gene expression, and that UL50-p26 regulates this pUL50 activity.

RESULTS

Expression of UL50-p26 from the UL50 gene. We previously observed that during infection with recombinant HCMV (AD169 strain) containing the C-terminally hemagglutinin (HA)-tagged UL50 gene (UL50-HA) (18), a smaller isoform of pUL50, which migrates in sodium dodecyl sulfate (SDS)-polyacrylamide gels at about 26 kDa (denoted here as UL50-p26), is expressed (17). To investigate the expression pattern of UL50-p26 during virus infection, human fibroblasts (HFs) were infected with the UL50-HA recombinant virus (Fig. 1A) at a multiplicity of infection (MOI) of 3, and immunoblot analysis was performed with an anti-HA antibody. pUL50 was expressed as early as 24 h after infection, and its expression reached a peak at 72 h under these conditions. We found that UL50-p26 was expressed earlier (12 h) than pUL50, showing a peak at 48 h, and became less abundant than pUL50 at later stages (72 and 96 h) of infection (Fig. 1B). This result suggests that the p26 isoform is expressed from the UL50 gene earlier than pUL50 but that UL50-p26 expression is downregulated during the late stages of virus infection. As reported previously (18), HA-tagged UL50 proteins accumulate at the nuclear rim at the late stages of infection (Fig. 1C).

Based on its estimated molecular weight in SDS-polyacrylamide gels, UL50-p26 appears to initiate from an internal methionine at amino acid position 199 in the UL50 gene, lacks the N-terminal globular domain responsible for binding pUL53, and retains
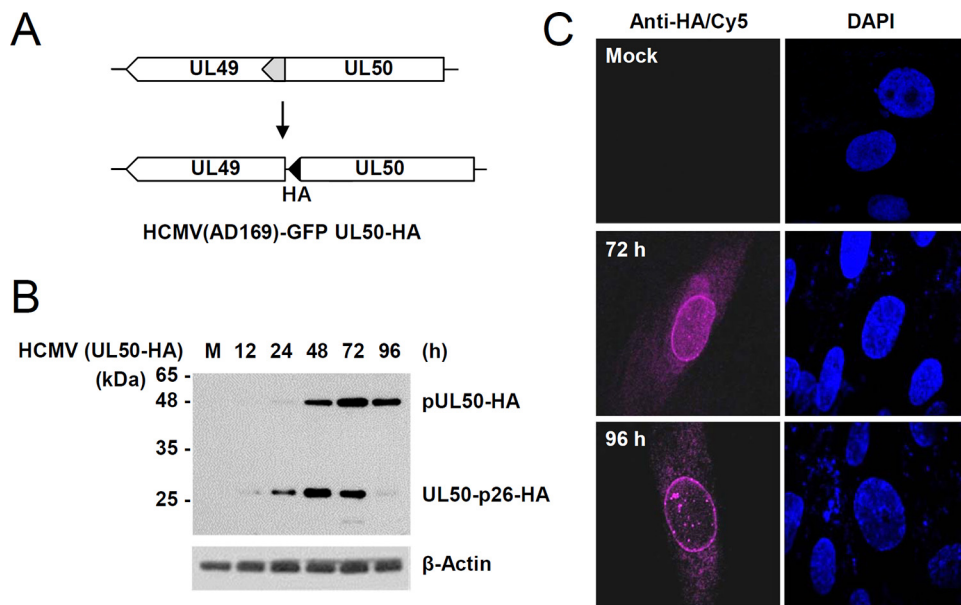
FIG 1 Detection of the p26 isoform encoded by the UL50 gene in HCMV-infected cells. (A) The scheme for UL50-HA virus production was described previously (18). In the UL50-HA virus, the overlapping region (gray) of UL49 and UL50 in the wild-type virus was duplicated and an HA tag (black) was specifically added at the end of UL50. (B) HF cells in six-well plates were mock infected (lane M) or infected with the UL50-HA virus at an MOI of 3. Cell lysates were prepared at the indicated time points, followed by immunoblotting with anti-HA and anti-IE1/IE2 (810R) antibodies. The levels of β-actin, which was used as a loading control, are shown. (C) HF cells in chamber slides were mock infected or infected with the UL50-HA virus for 72 or 96 h, and IFA was performed with an anti-HA antibody and a Cy5-labeled secondary antibody. Cell nuclei were stained with DAPI (4′,6-diamidino-2-phenylindole).

the transmembrane domain required for targeting the ER and the INM (Fig. 2A). To test this, a plasmid containing the UL50(M199V)-HA gene, in which methionine 199 of pUL50 was replaced with valine, was produced. Immunoblotting assays of plasmid DNA-transfected cells showed that, unlike the wild-type UL50-HA plasmid, the UL50(M199V)-HA plasmid did not express the p26 isoform, confirming that methionine 199 is the start site for UL50-p26 (Fig. 2B). When HF cells were transfected with a plasmid containing the gene for wild-type UL50-HA, UL50(M199V)-HA, or UL50-HA from residues 199 to 397 [UL50(199–397)-HA] and an indirect immunofluorescence assay (IFA) was performed with an anti-HA antibody, UL50-p26-HA was localized in the nuclear rim, although it was more cytoplasmic than pUL50-HA (Fig. 2C).

Delayed growth of the UL50(M199V) mutant virus and its correlation with reduced expression of IE2 and VCP/p97. To investigate the role of UL50-p26 during virus infection, we produced a recombinant virus (Toledo strain) containing the UL50(M199V) gene and its revertant virus using bacmid mutagenesis (Fig. 3A). Introduction of the mutation was confirmed by direct sequencing of the PCR products from the bacmid. When NcoI-digested bacmid DNA fragments were separated via agarose gel electrophoresis, the restriction enzyme-digested patterns of the wild-type, M199V mutant, and revertant bacmids did not show any apparent differences (data not shown), suggesting no gross alteration of the bacmid genomes. HF cells were infected with the wild-type, UL50(M199V) mutant, or revertant virus at an MOI of 0.5 or 0.1, and progeny virus titers in the culture supernatants were determined by infectious center assays. The UL50(M199V) virus showed slightly delayed growth at an MOI of 0.5, and this became more evident at an MOI of 0.1 (Fig. 3B).

We next examined the effect of UL50-p26 depletion on viral gene expression. HF cells were infected with the wild-type, UL50(M199V) mutant, or revertant virus at an MOI of 0.5, and the accumulation of viral proteins was analyzed at 1, 3, 5, or 7 days after infection by immunoblotting (Fig. 3C). At 3 days postinfection (dpi), the levels of IE2 (an immediate early protein) and p52 (an early protein) were lower in the UL50(M199V)
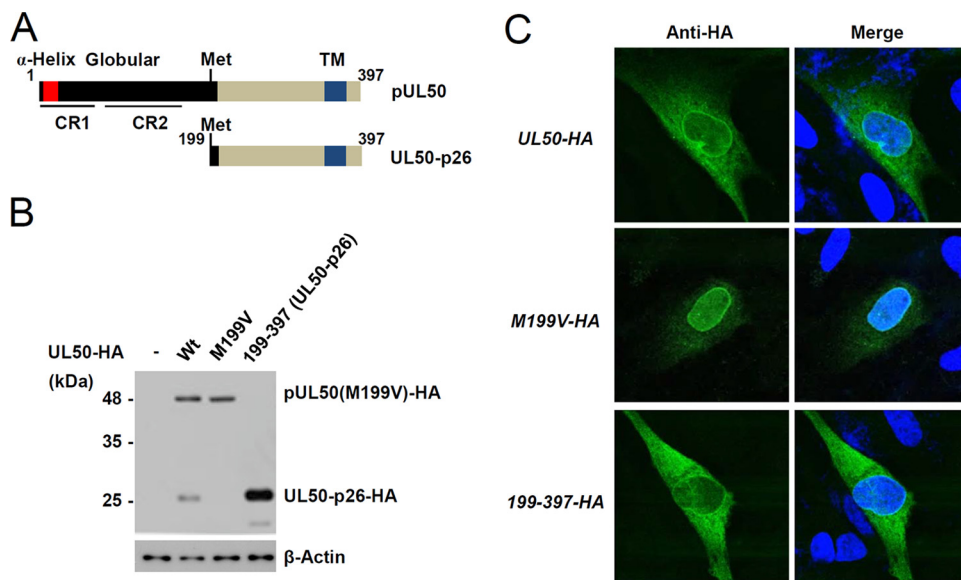
FIG 2 Identification of the internal methionine used for UL50-p26 expression. (A) Structures of pUL50 and UL50-p26. The α-helix, globular domain, and transmembrane (TM) regions are indicated. The relatively conserved regions (CR1 and CR2) in herpesvirus homologs are also indicated. (B) 293 cells in six-well plates were transfected with UL50 plasmids (1 μg) expressing the wild-type UL50-HA (Wt), UL50(M199V)-HA (M199V), or UL50(199−397)-HA gene, as indicated. At 48 h after transfection, cell lysates were prepared and immunoblotting was performed with anti-HA antibodies. The levels of β-actin, which was used as a loading control, are shown. (C) HF cells (1 $\times$ 10^5 cells) were electroporated with UL50 plasmids (1 μg). At 48 h after transfection, cells were fixed with 4% paraformalde-hyde and stained with an anti-HA antibody. Hoechst was used to stain the cell nuclei. Representative confocal laser scanning microscopic images are shown.

mutant virus than in the wild-type and revertant viruses; however, at 5 and 7 dpi, the levels of IE2, p52, and pp28 (a true late protein) became comparable among the three viruses. The lack of UL50-p26 expression in the UL50(M199V) mutant virus was also confirmed by immunoblotting with an anti-UL50 antibody.

Recently, valosin-containing protein (VCP; also known as p97 in mammals), a member of the ATPases associated with diverse cellular activities (AAA+) protein family (19), has been shown to play a critical role in IE2 expression by regulating alternative splicing of IE1 and IE2 mRNA transcripts during HCMV infection (20). This prompted us to compare VCP/p97 levels in virus-infected cells. During wild-type and revertant virus infection, VCP/p97 levels increased gradually as infection progressed; however, during UL50(M199V) mutant virus infection, the VCP/p97 level was reduced at 3 dpi and then became comparable to that in the wild-type and revertant viruses at 5 and 7 dpi (Fig. 3C). These immunoblot assay results suggest that delayed IE2 expression during UL50(M199V) virus infection might be related to altered VCP/p97 expression. Because pUL50 downregulates ISGylation by inducing UBE1L degradation, we also investigated whether the ISGylation level was affected. However, the overall ISGylation level was not significantly affected during mutant virus infection (Fig. 3C).

To further analyze the effect of UL50-p26 depletion on viral growth and VCP/p97 expression, we infected HF cells with the wild-type or UL50(M199V) mutant virus at an MOI of 3 or 0.05 and compared progeny virus titers and the levels of VCP/p97, IRE1, and UBE1L. IRE1 and UBE1L levels have been shown to be downregulated by pUL50 expression (16, 17). The growth of mutant virus was only slightly delayed at an MOI of 3, but it was significantly reduced at an MOI of 0.05, indicating an MOI-dependent growth defect of the mutant virus (Fig. 4A). At an MOI of 3, VCP/p97, IRE1, and UBE1L levels were all decreased at late times during wild-type virus infection. However, only VCP/p97 was effectively lost during mutant virus infection, suggesting that VCP/p97 may be regulated differently from IRE1 and UBE1L (Fig. 4B, left, and Fig. 4C, top). At an MOI of 0.05, the VCP/p97, IRE1, and UBE1L levels were all lower in the mutant virus than
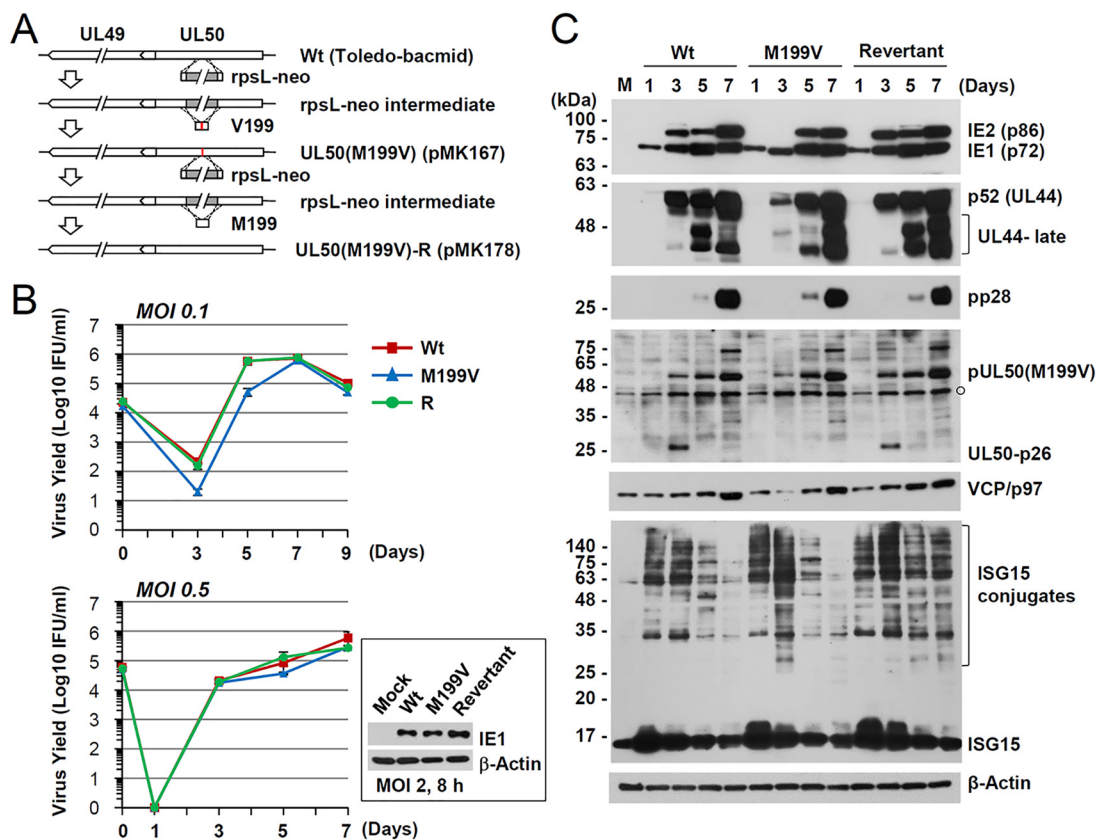
FIG 3 Production of the UL50(M199V) virus and comparison of its growth with that of the wild-type virus. (A) To construct the UL50(M199V) mutant bacmid clone, the *rpsL-neo* fragment with an homology arm was introduced by electroporation into *E. coli* DH10B containing the wild-type Toledo-bacmid. Intermediate bacmid clones were isolated based on resistance to kanamycin. The *rpsL-neo* fragment was replaced by annealed oligonucleotide DNAs that contained a replacement of the methionine at position 199 by valine (pMK167). The UL50(M199V) mutant bacmid was selected by streptomycin. Subsequently, the *rpsL-neo* fragment with an homology arm was again inserted into the mutant to construct its revertant. DNA fragments containing the wild-type UL50 gene were PCR amplified. The amplified UL50 gene was then swapped into the Toledo-bacmid containing the *rpsL-neo* cassette by homologous recombination (pMK178). (B) HF cells in 12-well plates were infected with Toledo viruses (wild-type, the M199V mutant, or the M199V revertant [R]) at an MOI of 0.5 or 0.1. The progeny virus titers in the culture supernatants were measured at the indicated time points after infection by infectious center assays. The results shown are mean values and standard errors from three independent experiments. IFU, infectious units. (C) HF cells were mock infected or infected at an MOI of 0.5, as described in the legend to panel B. Total cell lysates were prepared at the indicated time points and were subjected to SDS-PAGE and immunoblotting with antibodies to viral proteins (IE1/IE2, p52, pp28, and pUL50) and cellular proteins (VCP/p97 and ISG15). The levels of β-actin, which was used as a loading control, are shown.

in the wild-type virus and viral protein levels were significantly reduced in mutant virus infection (Fig. 4B, right, and Fig. 4C, bottom). Considering the very low level of pUL50 in cells infected with the mutant virus at an MOI of 0.05, it was not clear whether the decrease in VCP/p97, IRE1, and UBE1L levels was the direct effect of pUL50 expression (without UL50-p26) (Fig. 4B, right). However, these results generally support the idea that a lack of UL50-p26 expression affects viral growth at low MOIs and that low-level VCP/p97 accumulation may be at least partly related to the growth property of the mutant virus.

UL50 proteins regulate VCP/p97 stability and affect VCP/p97-mediated IE1/IE2 expression. Regulation of VCP/p97 expression by the UL50-encoded proteins was further investigated in human embryonic kidney (HEK) 293 cells using transient expression assays. Transfection of the UL50(M199V) plasmid expressing only pUL50(M199V) substantially reduced VCP/p97 expression, whereas transfection with the UL50(199–377) plasmid expressing UL50-p26 or the wild-type plasmid expressing both pUL50 and UL50-p26 did not (Fig. 5A). When the transmembrane domain was deleted from the wild-type UL50 gene expressing both pUL50 and UL50-p26, less UL50-p26(ΔTM) was expressed compared to the amount expressed in the wild-type plasmid, but VCP/p97
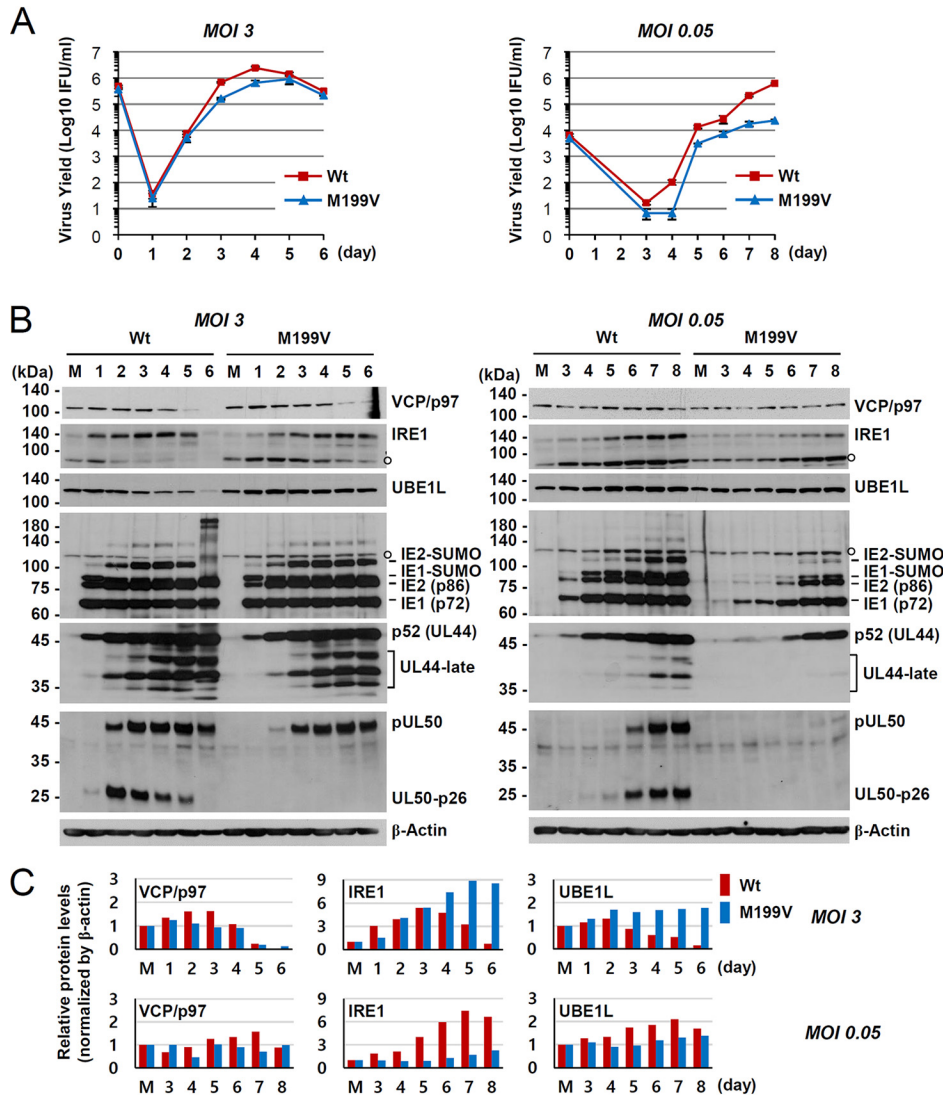
FIG 4 Comparison of viral growth and the effects of UL50-p26 on the levels of VCP/p97, IRE1, and UBE1L between wild-type and M199V mutant viruses. (A and B) HF cells in 12-well plates were infected with Toledo viruses (the wild type or M199V mutant) at an MOI of 3 or 0.05. Total cell lysates were prepared at the indicated time points, and progeny virus titers in the culture supernatants were measured by infectious center assays. (A) The results shown are mean values and standard errors from three independent experiments. (B) Total cell lysates were also prepared at the indicated time points and were subjected to SDS-PAGE, and immunoblotting was performed with antibodies to VCP/p97, IRE1, UBE1L, IE1/IE2, p52, pUL50, and β-actin. (C) VCP/p97, IRE1, and UBE1L levels normalized by the β-actin levels in panel B are shown.

expression was not reduced (Fig. 5A). This result suggests that pUL50 downregulates VCP/p97 in a manner dependent on the presence of its transmembrane domain but that UL50-p26 may negatively regulate this pUL50 activity. The effect of the pUL50(M199V) mutant on VCP/p97 may be due to the absence of UL50-p26 expression or may be due to the Met-to-Val substitution of the pUL50 protein. In similar cotransfection assays, the ability of pUL50(M199V) to downregulate VCP/p97 also required the presence of a transmembrane domain (Fig. 5B). These results indicate that targeting the membrane by pUL50 without UL50-p26 expression but not gaining the M199V mutation is critical for VCP/p97 downregulation. pUL50 expressed from adenoviral (Ad) vectors also reduced the level of endogenous VCP/p97 in a dose-dependent manner, but pUL50 did not reduce the VCP/p97 mRNA level, suggesting that the effect of pUL50 on VCP/p97 is posttranscriptional (Fig. 5C). In a control experiment, infection with similar input amounts of adenoviruses expressing β-galactosidase did not reduce
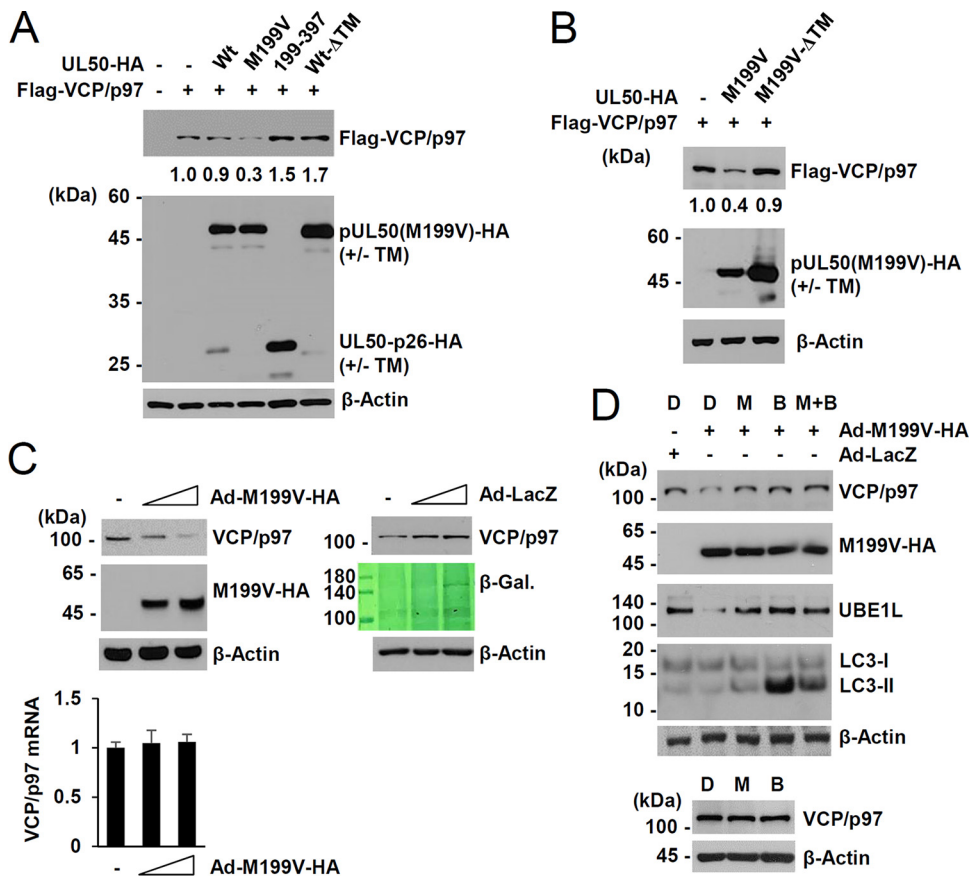
FIG 5 Effect of UL50 proteins on VCP/p97 expression in transfection assays. (A and B) 293 cells in six-well plates were cotransfected with plasmids (1 μg) expressing Flag-VCP/p97 or UL50-HA (wild type or mutants), as indicated. At 24 h after transfection, cell lysates were prepared and immunoblot assays were performed with anti-Flag or anti-HA antibodies. The levels of β-actin, which was used as a loading control, are shown. Relative Flag-VCP/p97 levels normalized to the levels of β-actin are indicated. (C) HF cells in 12-well plates (1.5×10^5 cells per well) were mock infected or infected with increasing amounts (3 and 6 50% tissue culture infective doses per cell) of recombinant adenoviruses expressing UL50(M199V)-HA or β-galactosidase (β-Gal.; LacZ), as indicated. Cells were harvested at 48 h after infection, and immunoblotting was performed with anti-VCP/p97, anti-HA, or anti-β-actin antibodies. Expression of β-galactosidase was determined by Coomassie blue staining. Transcript levels of VCP/p97 were also measured by RT-quantitative PCR. VCP/p97 mRNA levels normalized to those of β-actin are shown as a graph. (D) HF cells in 12-well plates (1.5×10^5 cells per well) were infected with recombinant adenoviruses, as described in the legend to panel C, at an MOI of 3. Cells were treated with sterile dimethyl sulfoxide (lane D), MG132 (20 μM; lane M), or bafilomycin A1 (100 nM; lane B) for 4 h, as indicated, prior to cell harvest at 60 h after infection. Cell lysates were prepared and subjected to immunoblotting with antibodies to VCP/p97, HA, UBE1L, LC3, or β-actin.

the level of VCP/p97. The pUL50-mediated loss of VCP/p97 was inhibited by the proteasome inhibitor MG132 and the lysosomal inhibitor bafilomycin A1 (Fig. 5D). MG132 and bafilomycin A1 treatment restored the pUL50-induced UBE1L loss, and bafilomycin A1 increased the lipid-modified form of LC3 (LC3-II), confirming the activities of the inhibitors. As a control, treatment with the inhibitors alone showed a minimal effect on VCP/p97 level. These results demonstrate that pUL50 downregulates VCP/p97 at the protein level in a transmembrane domain-dependent manner and that UL50-p26 may regulate this pUL50 activity.

Because VCP/p97 has been shown to promote IE2 expression by facilitating IE2 mRNA production by alternative splicing (20), we investigated whether UL50 proteins affect IE2 expression through VCP/p97 regulation. The pRL45 plasmid contains the major IE gene from the Towne strain (21). In cotransfection assays using pRL45, we found that VCP/p97 expression increased both IE1/IE2 expression and the IE1-to-IE2 transition (Fig. 6A, lanes 1 and 2). When plasmids containing the wild-type or mutant UL50 gene were compared, the UL50(M199V) plasmid expressing only pUL50(M199V)
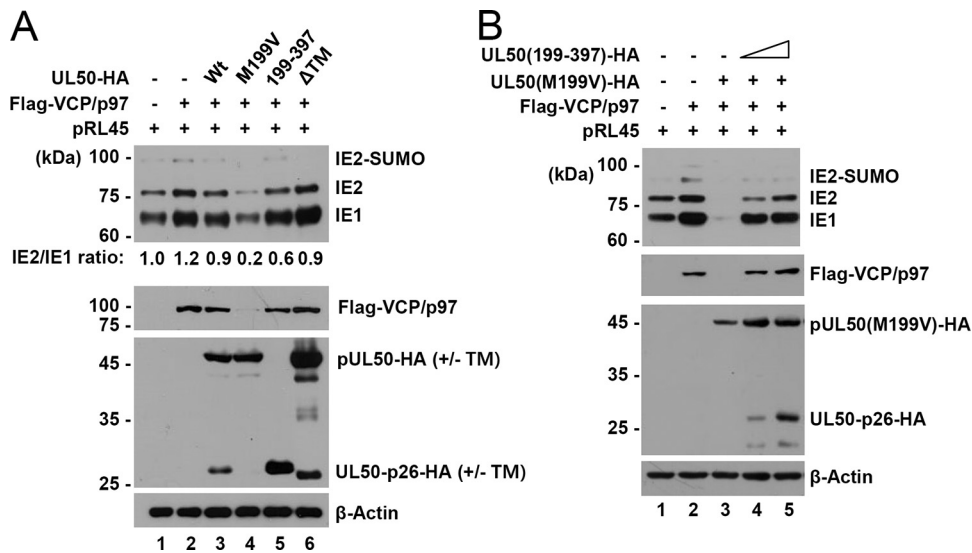
FIG 6 Effect of UL50-p26 on pUL50-mediated VCP/p97 loss and IE1/IE2 downregulation. (A) 293 cells in six-well plates were cotransfected with the pRL45 plasmid containing the MIE gene (0.5 μg), a plasmid expressing Flag-VCP/p97 (0.5 μg), and a plasmid (0.5 μg) containing the UL50-HA gene (wild type or mutants), as indicated. At 24 h after cotransfection, cell lysates were prepared and immunoblotting analysis was performed with anti-810R (for IE1/IE2), anti-HA, anti-Flag, or anti-β-actin (as a loading control) antibodies. Relative IE2/IE1 ratios are indicated. (B) 293 cells in six-well plates were cotransfected with the pRL45 plasmid (0.25 μg), a plasmid (0.5 μg) expressing Flag-VCP/p97 or pUL50 [UL50(M199V)-HA], and increasing amounts (0.125 or 0.25 μg) of a plasmid expressing UL50-p26-HA [UL50(199–397)-HA], as indicated. At 24 h after cotransfection, cell lysates were prepared and immunoblotting analysis was performed as described in the legend to panel A.

led to a reduction in the VCP/p97 level and IE1/IE2 expression, whereas the UL50(199–397) plasmid expressing UL50-p26 did not (Fig. 6A, lanes 4 and 5). Interestingly, the wild-type UL50 plasmid expressing both UL50 proteins (either the intact or the ΔTM mutant form) did not significantly affect the VCP/p97 level or IE1/IE2 expression (Fig. 6A, lanes 3 and 6). These cotransfection assay results demonstrate that VCP/p97 destabilization by pUL50 inhibits both IE1/IE2 expression and the IE1-to-IE2 transition and also support the notion that UL50-p26 has a regulatory role in pUL50-mediated VCP/p97 loss.

To directly address the effect of UL50-p26 on pUL50-mediated VCP/p97 loss, we performed a competition assay in 293 cells. Consistent with earlier observations, VCP/p97 enhanced IE1/IE2 expression from pRL45 and pUL50 inhibited VCP/p97 expression, leading to a substantial reduction in IE1/IE2 expression (Fig. 6B, lanes 1 to 3); however, coexpression of UL50-p26 dose-dependently inhibited pUL50-mediated VCP/p97 loss and restored IE1/IE2 levels (Fig. 6B, lanes 4 and 5). These competition assay results clearly demonstrate that UL50-p26 has an inhibitory effect on pUL50-mediated VCP/p97 loss.

UL50-p26 interferes with the pUL50-VCP/p97 interaction. We next investigated the mechanism by which UL50-p26 inhibits pUL50-mediated VCP/p97 loss. 293T cells were cotransfected with a plasmid expressing Flag-VCP/p97 and a plasmid containing the wild-type or mutant UL50-HA gene, and coimmunoprecipitation (co-IP) assays were performed. We found that both pUL50 and UL50-p26 could interact with VCP/p97, although UL50-p26 showed much weaker VCP/p97 binding than pUL50, and their TM deletion mutants did not interact with VCP/p97 (Fig. 7A). The association of UL50 proteins with VCP/p97 was further assessed by IFA. In transfected HeLa cells, Flag-VCP/p97 was both nuclear and cytoplasmic, while UL50 proteins accumulated at the nuclear rim, as expected (Fig. 7B). When cotransfected, Flag-VCP/p97 colocalized at the nuclear rim more effectively with pUL50 than with UL50-p26, which might reflect the different strengths of binding of pUL50 versus UL50-p26 to VCP/p97 (Fig. 7C). These IFA results support the idea that pUL50 interacts more effectively with VCP/p97 than with UL50-p26.
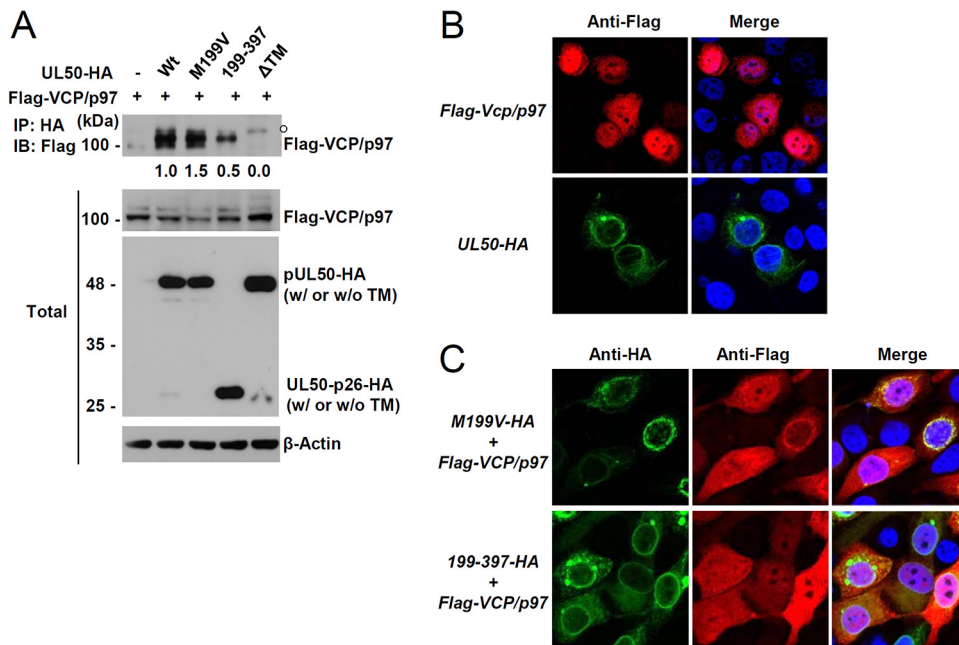
FIG 7 Interaction of pUL50 with VCP/p97. (A) 293T cells in six-well plates were cotransfected with a plasmid (1 μg) encoding Flag-VCP/p97 and a plasmid (0.7 μg) expressing wild-type or mutant UL50-HA, as indicated. At 24 h after transfection, cell lysates were prepared and immunoprecipitated (IP) with an anti-HA antibody, followed by immunoblotting (IB) with an anti-Flag antibody. The expression level of each protein in the total cell lysates was also determined by immunoblotting. The levels of β-actin, which was used as a loading control, are shown. The amounts of coimmunoprecipitated Flag-VCP/p97 protein normalized by the input amount of protein (also normalized by the amount of UL50-HA protein and β-actin) were quantitated. (B and C) HeLa cells in four-well chamber slides were transfected with a plasmid expressing Flag-VCP/p97 or expressing the UL50-HA gene (B) or cotransfected with a plasmid expressing Flag-VCP/p97 and a plasmid expressing the UL50(M199V)-HA or UL50(199–397)-HA gene (C), as indicated. At 48 h after transfection, the cells were fixed with 4% paraformaldehyde and stained with anti-HA and anti-Flag antibodies. Hoechst was used to stain cell nuclei. Representative confocal laser scanning microscopic images are shown.

KSHV ORF67, a homolog of pUL50, has been shown to self-interact, and this interaction is promoted by the presence of the transmembrane domain (22). We investigated whether pUL50 and UL50-p26 can interact with each other. 293T cells were cotransfected with HA- or SRT-tagged UL50 proteins, and co-IP assays were performed. We found that pUL50 interacted with itself and UL50-p26, but the binding strength between pUL50 and UL50-p26 was 6-fold stronger than that between pUL50 and itself, and these interactions between UL50 proteins required the transmembrane domain (Fig. 8A). These results suggest that UL50-p26 may have a protective effect on pUL50-mediated VCP/p97 loss by interfering with the interaction between pUL50 and VCP/p97. To address this question, we performed competitive co-IP assays and found that the interaction of pUL50 with VCP/p97 was indeed inhibited by UL50-p26 in a dose-dependent manner (Fig. 8B). These results strongly support the notion that UL50-p26 inhibits pUL50-mediated VCP/p97 loss by interfering with the pUL50-VCP/p97 interaction.

DISCUSSION

In this study, we demonstrated that a smaller isoform of pUL50, UL50-p26, is expressed during HCMV infection from an internal methionine codon in the UL50 gene. A mutant virus that lacked UL50-p26 expression showed a growth defect at low MOIs, and this correlated with the reduced expression of IE2 and VCP/p97. Considering the positive role of VCP/p97 in IE2 expression (20), one of the roles of UL50-p26 may be to promote efficient VCP/p97 expression. Interestingly, we discovered that pUL50 could induce the loss of VCP/p97 and that UL50-p26 could inhibit this pUL50 activity by associating with pUL50.
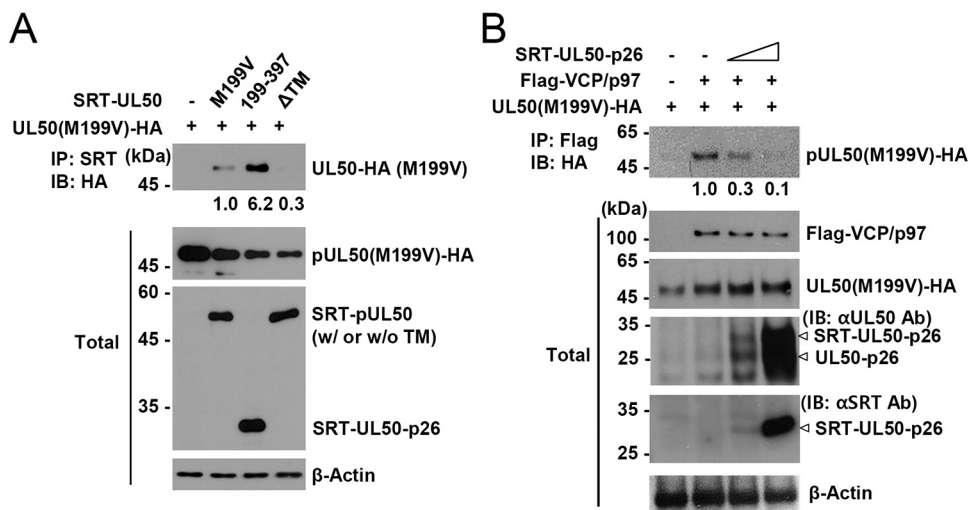
FIG 8 Inhibition of the pUL50-VCP/p96 interaction by UL50-p26. (A) 293T cells in six-well plates were cotransfected with a plasmid (1 μg) containing the UL50(M199V)-HA gene and a plasmid (1 μg) expressing SRT-UL50 (M199V, 199–397, or ΔTM), as indicated. At 24 h after transfection, cell lysates were prepared and immunoprecipitated with an anti-SRT antibody, followed by immunoblotting with an anti-HA antibody. The expression level of each protein in total cell lysates was also determined by immunoblotting. The levels of β-actin, which was used as a loading control, are shown. The relative binding strength of the UL50 proteins normalized by the amounts of VCP/p97, UL50 proteins, and β-actin in total cell lysates are shown. (B) 293T cells in six-well plates were cotransfected with a plasmid (0.7 μg) containing the UL50(M199V)-HA gene and a plasmid (1.3 μg) expressing Flag-VCP/p97 and increasing amounts (0.25 and 0.5 μg) of plasmid expressing SRT-UL50-p26, as indicated. At 24 h after transfection, cell lysates were prepared and immunoprecipitated with an anti-Flag antibody, followed by immunoblotting with an anti-HA antibody. The expression level of each protein in total cell lysates was also determined by immunoblotting. The levels of β-actin, which was used as a loading control, are shown. The relative binding strength of UL50(M199V)-HA to Flag-VCP/p97 normalized by the amount of input protein and β-actin is indicated. Ab, antibody.

The downregulation of VCP/p97 by pUL50 was unexpected. Given that VCP/p97 promotes viral gene expression, the ability of UL50-p26 to inhibit pUL50-mediated VCP/p97 loss appears to be beneficial for viral gene expression. However, VCP/p97 is a multifunctional protein involved in various cellular processes and the ER-associated degradation (ERAD) pathway in particular (23, 24). VCP/p97 has a globular N-terminal domain, two AAA ATPase domains (D1 and D2), and a C-terminal tail. The N- and C-terminal domains interact with diverse substrates and with cofactors involved in ubiquitin-proteasome-mediated protein degradation (24–26). In the ERAD pathway, a substrate is conjugated with ubiquitin by an E3 ligase on the cytoplasmic side of the ER membrane. The VCP/p97-Ufd1-Npl4 complex is then recruited to the membrane to extract the substrate for degradation by the proteasome (25–27). Therefore, it is also possible that pUL50-mediated VCP/p97 loss regulates the ERAD pathway and that HCMV has evolved to finely regulate these pUL50-associated activities by expressing a small isoform of pUL50.

How pUL50 induces VCP/p97 loss is unclear. Our analysis using inhibitors suggests that VCP/p97 loss may occur through both proteasomal and lysosomal pathways. pUL50 has been shown to induce the loss of IRE1 and inhibit the UPR, although the underlying mechanism has not been addressed (16). We previously showed that pUL50 induces UBE1L degradation. Of note, this UBE1L degradation is ubiquitin and proteasome dependent and is promoted by the interaction of pUL50 with RNF170, an ubiquitin E3 ligase (17). Therefore, it is possible that the pUL50-mediated VCP/p97 loss at least partly involves RNF170. Although our analysis suggested that VCP/p97 may be regulated differently from IRE1 and UBE1L, further investigation into the roles of UL50-p26 in IRE1 and UBE1L regulation is necessary.

Interestingly, VCP/p97, IRE1, and UBE1L loss required the membrane-targeting ability of pUL50. In this regard, it is notable that KSHV ORF67 and EBV BFRF1, which are homologs of HCMV pUL50, are able to induce membrane proliferation (9, 11, 22, 28).

This membrane-proliferative activity may be associated with the unexpected NEC-independent function of pUL50. The ER network plays key roles in metabolism and cellular organization and dynamically alters the morphology and composition of cells. ER proliferation by viral proteins may induce cellular homeostatic responses, such as activation of unconventional protein secretion pathways and ER-phagy (29, 30). The loss of VCP/p97 may be related to these cellular responses. In fact, we observed that pUL50 overexpression resulted in VCP/p97 secretion into the culture supernatants of cotransfected cells (data not shown). Given that UL50-p26 expression precedes pUL53 expression, this early expression of UL50-p26 may be necessary to control the membrane-proliferating and associated activities of pUL50. Of note, our analysis with wild-type and M199V mutant viruses showed that the changes in VCP/p97 levels did not always correlate with the expression kinetics of pUL50 at late stages. In particular, although only pUL50 was expressed at very late stages of wild-type and mutant virus infection at an MOI of 0.5 (Fig. 3C), VCP levels were still high. Why the VCP/p97 level was not affected at this time point is not clear. However, it is conceivable that pUL50 may transiently affect the VCP level only during targeting of the ER before it associates with pUL53 in the nuclear rim at very late stages.

Lin et al. were the first to identify VCP/p97 as a positive regulator of IE2 synthesis during HCMV infection (20). Specifically, they showed that VCP/p97 is required for efficient switching of splicing from exons 3 and 4 (for IE1 production) to exons 4 and 5 (for IE2 production). Interestingly, when we used a genomic clone containing the MIE gene in cotransfection assays, VCP/p97 expression was required not only for the transition from IE1 to IE2 production but also for IE1 expression (Fig. 6). When we infected cells with the mutant virus at an MOI of 0.5, VCP/p97 downregulation by the lack of UL50-p26 expression affected only IE2 production (Fig. 3C), which is consistent with the observations of Lin et al. in VCP/p97-depleted cells (20). The different effects of VCP/p97 expression on IE1 and IE2 expression in transfected and virus-infected cells need further investigation.

MATERIALS AND METHODS

Cell culture, transfection, and inhibitors. HF, HEK 293, 293T, and 293A, and HeLa cells were grown in Dulbecco's modified Eagle's medium supplemented with 10% fetal bovine serum, penicillin (100 U/ml), and streptomycin (100 μg/ml). Nonessential amino acids (NEAA) were also added to the medium for HEK 293A cells. DNA transfection of 293, 293T, 293A, and HeLa cells was performed using the polyethyleneimine (PEI) version of the cationic polymer procedure (31). The proteasome inhibitor MG132 and the lysosome inhibitor bafilomycin A1 were purchased from Sigma.

Viruses. Recombinant HCMV (Toledo strain) was produced by transfecting a Toledo-bacmid, a gift from Hua Zhu (UMDNJ-New Jersey Medical School), into HF cells (32). HCMV (AD169 strain)-green fluorescent protein (GFP) UL50-HA (18) was provided by Manfred Marshall (Friedrich-Alexander University of Erlangen-Nürnberg) and grown in HF cells. UV-inactivated viruses were produced by irradiating the virus stock with UV light three times at 0.72 J/cm² using a CL-1,000 cross-linker (UVP).

Infectious center assay. Diluted samples were used to inoculate a monolayer of 4×10^4 HF cells in a 24-well plate. At 24 h postinfection, cells were fixed with 500 μl of cold methanol for 10 min. The cells were then washed three times in phosphate-buffered saline (PBS) and incubated with an anti-IE1 rabbit polyclonal antibody in PBS at 37°C for 1 h, followed by incubation with phosphatase-conjugated anti-rabbit immunoglobulin G (IgG) antibody in PBS at 37°C for 1 h. Finally, the cells were gently washed in PBS and treated with 200 μl of developing solution (nitroblue tetrazolium, 5-bromo-4-chloro-3-indolylphosphate) at room temperature for 1 h. Positively stained cells were counted in five separate fields per well under a light microscope (magnification, ×200).

Expression plasmids and adenoviral vectors. Mammalian expression plasmids for pcDNA3.1-UL50-HA were described previously (12). The following mutant versions of pcDNA3.1-UL50-HA were produced using mutagenesis with a Stratagene QuikChange site-directed mutagenesis kit: M199V (pMK113), residues 199 to 397 (pMK94), deletion of the TM domain from residues 358 to 381 (ΔTM) (pMK183), and M199V with ΔTM (pMK275). VCP/p97 was PCR amplified from a plasmid expressing Myc-VCP/p97, a gift from Jae Hyuk Shim (Cornell University), and subcloned into the pENTR vector (Invitrogen). The pSG5 (33) plasmid expressing Flag-VCP/p97 (pMK257) was produced by transferring the DNA to pSG5 using LR Clonase (Invitrogen). Plasmid pRL45, expressing both IE1 and IE2 under the control of their endogenous transcriptional and splicing signals, was described previously (34). The plasmid expressing HA-ubiquitin (HA-Ub) was described previously (32). The following wild-type and mutant versions of pCMV6-SRT-UL50 were produced using mutagenesis with a Stratagene QuikChange site-directed mutagenesis kit: wild type (pMK55), M199V (pMK268), residues 199 to 397 (pMK269), and deletion of the TM domain from residues 358 to 381 (ΔTM) (pMK263).

Adenoviral vectors expressing pUL50(M199V)-HA (pMK270) were produced in pAD/CMV/V5-DEST (Invitrogen) by transferring DNA using LR Clonase. Recombinant adenoviruses were grown in 293A cells after transfection with adenoviral vector DNAs that were linearized by PacI restriction enzyme digestion. A control adenoviral vector expressing β-galactosidase (Ad-lacZ) was obtained from Invitrogen.

Bacmid mutagenesis. The HCMV (Toledo)-bacmid containing the UL50(M199V) gene was generated using a counterselection bacterial artificial chromosome (BAC) modification kit (Gene Bridges, Germany). Briefly, rpsL-neo cassettes flanked by 100 nucleotides upstream and downstream of the target site [UL50(M199V)] were PCR amplified using the following primer set: LMV2014 (5′-GCT GTA CGC CAA GAA AGC CGC GTC GAC GTC GTT GGC GGT CCG GAA CCA CGG GCC TGG TGA TGA TGG CGG GAT CG-3′) and LMV2015 (5′-CCG CAT CGT CCC ATA CAG GCC TCA CAA CGA CAC AGC CGC CAC GAC CCC GCT CAG AAG AAC TCG TCA AGA AGG CG-3′). The amplified rpsL-neo fragments were purified and introduced into Escherichia coli DH10B containing wild-type Toledo-bacmid for recombination via electroporation using a Gene Pulser II system (Bio-Rad). The intermediate Toledo-bacmid construct containing the rpsL-neo cassette was selected on Luria broth (LB) agar plates containing kanamycin. Next, M199V DNA fragments to replace the rpsL-neo cassette were PCR amplified using primers LMV2016 (5′-GCT GTA CGC CAA GAA AGC CGC GTC GAC-3′) and LMV2017 (5′- CCG CAT CGT CCC ATA CAG GCC TCA CAA-3′) with the pMK113 plasmid as the template. Amplified fragments were recombined into Toledo-bacmid containing the rpsL-neo cassette, and E. coli cells containing the UL50(M199V) bacmid were selected on LB plates containing streptomycin. Mutated regions were amplified and sequenced to verify the presence of the desired mutations. To generate the revertant Toledo-bacmid from the mutant, DNA fragments containing the wild-type target gene were PCR amplified and inserted into the mutant Toledo-bacmid by homologous recombination as described above. To grow recombinant viruses, Toledo-bacmids were introduced into HF cells by electroporation. For each reaction, HF cells (2 × 10⁶) in 600 μl of resuspension buffer were mixed with 5 μl of Toledo-BAC DNA, 4.5 μl of a plasmid encoding transactivator pp71, and 0.5 μl of pEGFP-C1 to monitor the electroporation efficiency. After electroporation for 35 ms at 1,350 V using a Microporator MP-100 apparatus (Digital Bio Technology), cells were plated in T-25 flasks.

Antibodies. Anti-HA rat monoclonal antibody (MAb) 3F10 and anti-Myc mouse MAb 9E10 conjugated with horseradish peroxidase (HRP) or labeled with fluorescein isothiocyanate (FITC) were purchased from Roche. Mouse MAbs against UL44 (p52) and UL99 (pp28) were obtained from Virusys. Mouse MAb 810R against IE1 and IE2 was purchased from Chemicon. Anti-β-actin and anti-Flag mouse MAbs were purchased from Sigma. Mouse MAb against the SRT epitope has been described previously (35). Anti-ISG15 (F-9), anti-IRE1α (B-12), and anti-VCP/p97 (D-9) mouse MAbs were obtained from Santa Cruz. Rabbit antipeptide polyclonal antibody (PAb) for pUL50 was described previously (17). Rabbit PAb for UBE1L was obtained from Abcam.

Indirect immunofluorescence assay (IFA). Cells in chamber slides were fixed in 4% paraformaldehyde for 5 min and permeabilized in PBS containing 0.2% Triton X-100 for 20 min at 4°C. The cells were then incubated with appropriate primary antibodies (anti-HA at a 1:200 dilution, anti-Flag at a 1:2,000 dilution) in PBS for 1 h at 37°C, followed by incubation with appropriate secondary antibodies at a 1:100 dilution for 1 h at 37°C. An FITC-conjugated anti-HA antibody (Roche) was also used at a 1:100 dilution. For double labeling, two different antibodies were incubated together. Cy5- or rhodamine-labeled secondary antibodies (Jackson ImmunoResearch) were used at a 1:100 dilution. Mounting solution containing Hoechst stain and antifade reagent (Molecular Probes) was used. Slides were examined and photographed with a Carl Zeiss LSM710 Meta confocal microscope system.

Immunoblot analysis. Cells were washed with phosphate-buffered saline (PBS), and total cell lysates were prepared by boiling the cell pellets in sodium dodecyl sulfate (SDS) loading buffer. Equal amounts of clarified cell extracts were separated on an SDS-polyacrylamide gel and electroblotted onto nitrocellulose membranes. The blots were blocked with PBS plus 0.1% Tween 20 (PBST) containing 5% nonfat dry milk and incubated for 1 h at room temperature. After three washes with PBST, the blots were incubated with appropriate antibodies in PBST for 1 h at room temperature. Antibody dilutions were 1:5,000 for anti-p52 (UL44), anti-pp28 (UL99), anti-β-actin, anti-IRE1α, and anti-VCP/p97; 1:2,500 for anti-Flag and 810R; 1:10,000 for anti-SRT and anti-UBE1L; and 1:1,000 for anti-UL50 and anti-ISG15 antibodies. After three 5-min washes with PBST, the blots were incubated with HRP-conjugated goat anti-mouse IgG or anti-rabbit IgG (Amersham) at a 1:5,000 dilution for 1 h at room temperature. An HRP-conjugated anti-HA antibody was used at a 1:5,000 dilution. The blots were then washed three times with PBST, and the protein bands were visualized with an enhanced chemiluminescence system (Amersham). Relative protein levels in the immunoblots were quantitated using ImageJ software (NIH).

Coimmunoprecipitation assay. Cell lysates were prepared by sonication in 1 ml co-IP buffer (50 mM Tris-Cl [pH 7.4], 50 mM NaF, 5 mM sodium phosphate, 150 mM NaCl, 0.1% NP-40, protease inhibitors [Sigma]) with a Vibra-Cell microtip probe (Sonics and Materials) for 10 s (pulse on for l s, pulse off for 3 s). Cell lysates were incubated with appropriate antibodies (10 μg) for 16 h at 4°C. Next, 30 μl of a 50% slurry of protein A- and protein G-Sepharose (Amersham) was added, and the mixture was incubated for 2 h at 4°C to allow adsorption. The mixture was then pelleted and washed seven times with co-IP buffer. The beads were resuspended and boiled for 5 min in loading buffer. Each sample was analyzed by SDS-polyacrylamide gel electrophoresis (PAGE) and immunoblotting with appropriate antibodies.

Reverse transcription (RT)-PCR. Total RNAs were isolated from virus-infected cells using the TRIzol reagent (Molecular Research Center, Inc.) and a MaXtract high-density tube (Qiagen). cDNAs were synthesized using the random hexamer/oligo(dT) primers provided in the QuantiTect reverse transcriptase kit (Qiagen). PCR was performed using the following primers: VCP/p97 forward (5′-AAACCGTGGTA GAGGTGCCA-3′), VCP/p97 reverse (5′-CTTGGAAGGTGTCATGCCAA-3′), β-actin forward (5′-AGCGGGAAA TCGTGCGTG-3′), and β-actin reverse (5′-CAGGGTACATGGTGGTGCC-3′).

ACKNOWLEDGMENTS

REFERENCES

1. Marschall M, Muller YA, Diewald B, Sticht H, Milbradt J. 2017. The human cytomegalovirus nuclear egress complex unites multiple functions: recruitment of effectors, nuclear envelope rearrangement, and docking to nuclear capsids. Rev Med Virol 27:e1934. https://doi.org/10.1002/rmv.1934.

2. Johnson DC, Baines JD. 2011. Herpesviruses remodel host membranes for virus egress. Nat Rev Microbiol 9:382–394. https://doi.org/10.1038/nrmicro2559.

3. Hellberg T, Paßvogel L, Schulz KS, Klupp BG, Mettenleiter TC. 2016. Nuclear egress of herpesviruses: the prototypic vesicular nucleocytoplasmic transport. Adv Virus Res 94:81–140. https://doi.org/10.1016/bs.aivir.2015.10.002.

4. Lye MF, Wilkie AR, Filman DJ, Hogle JM, Coen DM. 2017. Getting to and through the inner nuclear membrane during herpesvirus nuclear egress. Curr Opin Cell Biol 46:9–16. https://doi.org/10.1016/j.ceb.2016.12.007.

5. Bigalke JM, Heldwein EE. 2017. Have NEC coat, will travel: structural basis of membrane budding during nuclear egress in herpesviruses. Adv Virus Res 97:107–141. https://doi.org/10.1016/bs.aivir.2016.07.002.

6. Milbradt J, Auerochs S, Sticht H, Marschall M. 2009. Cytomegaloviral proteins that associate with the nuclear lamina: components of a postulated nuclear egress complex. J Gen Virol 90:579–590. https://doi.org/10.1099/vir.0.005231-0.

7. Sam MD, Evans BT, Coen DM, Hogle JM. 2009. Biochemical, biophysical, and mutational analyses of subunit interactions of the human cytomegalovirus nuclear egress complex. J Virol 83:2996–3006. https://doi.org/10.1128/JVI.02441-08.

8. Klupp BG, Granzow H, Fuchs W, Keil GM, Finke S, Mettenleiter TC. 2007. Vesicle formation from the nuclear membrane is induced by coexpression of two conserved herpesvirus proteins. Proc Natl Acad Sci U S A 104:7241–7246. https://doi.org/10.1073/pnas.0701757104.

9. Gonnella R, Farina A, Santarelli R, Raffa S, Feederle R, Bei R, Granato M, Modesti A, Frati L, Delecluse HJ, Torrisi MR, Angeloni A, Faggioni A. 2005. Characterization and intracellular localization of the Epstein-Barr virus protein BFLF2: interactions with BFRF1 and with the nuclear lamina. J Virol 79:3713–3727. https://doi.org/10.1128/JVI.79.6.3713-3727.2005.

10. Farina A, Feederle R, Raffa S, Gonnella R, Santarelli R, Frati L, Angeloni A, Torrisi MR, Faggioni A, Delecluse HJ. 2005. BFRF1 of Epstein-Barr virus is essential for efficient primary viral envelopment and egress. J Virol 79:3703–3712. https://doi.org/10.1128/JVI.79.6.3703-3712.2005.

11. Santarelli R, Farina A, Granato M, Gonnella R, Raffa S, Leone L, Bei R, Modesti A, Frati L, Torrisi MR, Faggioni A. 2008. Identification and characterization of the product encoded by ORF69 of Kaposi's sarcoma-associated herpesvirus. J Virol 82:4562–4572. https://doi.org/10.1128/JVI.02400-07.

12. Milbradt J, Auerochs S, Marschall M. 2007. Cytomegaloviral proteins pUL50 and pUL53 are associated with the nuclear lamina and interact with cellular protein kinase C. J Gen Virol 88:2642–2650. https://doi.org/10.1099/vir.0.82924-0.

13. Sonntag E, Hamilton ST, Bahsi H, Wagner S, Jonjic S, Rawlinson WD, Marschall M, Milbradt J. 2016. Cytomegalovirus pUL50 is the multi-interacting determinant of the core nuclear egress complex (NEC) that recruits cellular accessory NEC components. J Gen Virol 97:1676–1685. https://doi.org/10.1099/jgv.000495.

14. Sonntag E, Milbradt J, Svrlanska A, Strojan H, Hage S, Kraut A, Hesse AM, Amin B, Sonnewald U, Coute Y, Marschall M. 2017. Protein kinases responsible for the phosphorylation of the nuclear egress core complex of human cytomegalovirus. J Gen Virol 98:2569–2581. https://doi.org/10.1099/jgv.000931.

15. Sharma M, Coen DM. 2014. Comparison of effects of inhibitors of viral and cellular protein kinases on human cytomegalovirus disruption of nuclear lamina and nuclear egress. J Virol 88:10982–10985. https://doi.org/10.1128/JVI.01391-14.

16. Stahl S, Burkhart JM, Hinte F, Tirosh B, Mohr H, Zahedi RP, Sickmann A, Ruzsics Z, Budt M, Brune W. 2013. Cytomegalovirus downregulates IRE1 to repress the unfolded protein response. PLoS Pathog 9:e1003544. https://doi.org/10.1371/journal.ppat.1003544.

17. Lee MK, Kim YJ, Kim YE, Han TH, Milbradt J, Marschall M, Ahn JH. 2018. Transmembrane protein pUL50 of human cytomegalovirus inhibits ISGylation by downregulating UBE1L. J Virol 92:e00462-18. https://doi.org/10.1128/JVI.00462-18.

18. Schmeiser C, Borst E, Sticht H, Marschall M, Milbradt J. 2013. The cytomegalovirus egress proteins pUL50 and pUL53 are translocated to the nuclear envelope through two distinct modes of nuclear import. J Gen Virol 94:2056–2069. https://doi.org/10.1099/vir.0.052571-0.

19. Meyer H, Weihl CC. 2014. The VCP/p97 system at a glance: connecting cellular function to disease pathogenesis. J Cell Sci 127:3877–3883. https://doi.org/10.1242/jcs.093831.

20. Lin YT, Prendergast J, Grey F. 2017. The host ubiquitin-dependent segregase VCP/p97 is required for the onset of human cytomegalovirus replication. PLoS Pathog 13:e1006329. https://doi.org/10.1371/journal.ppat.1006329.

21. Pizzorno MC, O'Hare P, Sha L, LaFemina RL, Hayward GS. 1988. trans-Activation and autoregulation of gene expression by the immediate-early region 2 gene products of human cytomegalovirus. J Virol 62:1167–1179. https://doi.org/10.1128/JVI.62.4.1167-1179.1988.

22. Luitweiler EM, Henson BW, Pryce EN, Patel V, Coombs G, McCaffery JM, Desai PJ. 2013. Interactions of the Kaposi's sarcoma-associated herpesvirus nuclear egress complex: ORF69 is a potent factor for remodeling cellular membranes. J Virol 87:3915–3929. https://doi.org/10.1128/JVI.03418-12.

23. Meyer H, Bug M, Bremer S. 2012. Emerging functions of the VCP/p97 AAA-ATPase in the ubiquitin system. Nat Cell Biol 14:117–123. https://doi.org/10.1038/ncb2407.

24. van den Boom J, Meyer H. 2018. VCP/p97-mediated unfolding as a principle in protein homeostasis and signaling. Mol Cell 69:182–194. https://doi.org/10.1016/j.molcel.2017.10.028.

25. Stolz A, Hilt W, Buchberger A, Wolf DH. 2011. Cdc48: a power machine in protein degradation. Trends Biochem Sci 36:515–523. https://doi.org/10.1016/j.tibs.2011.06.001.

26. Ye Y, Tang WK, Zhang T, Xia D. 2017. A mighty "protein extractor" of the cell: structure and function of the p97/CDC48 ATPase. Front Mol Biosci 4:39. https://doi.org/10.3389/fmolb.2017.00039.

27. Stach L, Freemont PS. 2017. The AAA+ ATPase p97, a cellular multitool. Biochem J 474:2953–2976. https://doi.org/10.1042/BCJ20160783.

28. Desai PJ, Pryce EN, Henson BW, Luitweiler EM, Cothran J. 2012. Reconstitution of the Kaposi's sarcoma-associated herpesvirus nuclear egress complex and formation of nuclear membrane vesicles by coexpression of ORF67 and ORF69 gene products. J Virol 86:594–598. https://doi.org/10.1128/JVI.05988-11.

29. Rabouille C. 2017. Pathways of unconventional protein secretion. Trends Cell Biol 27:230–240. https://doi.org/10.1016/j.tcb.2016.11.007.

30. Wilkinson S. 2019. ER-phagy: shaping up and destressing the endoplasmic reticulum. FEBS J 286:2645–2663. https://doi.org/10.1111/febs.14932.

31. Boussif O, Lezoualc'h F, Zanta MA, Mergny MD, Scherman D, Demeneix B, Behr JP. 1995. A versatile vector for gene and oligonucleotide transfer into cells in culture and in vivo: polyethylenimine. Proc Natl Acad Sci U S A 92:7297–7301. https://doi.org/10.1073/pnas.92.16.7297.

32. Kwon KM, Oh SE, Kim YE, Han TH, Ahn JH. 2017. Cooperative inhibition

of RIP1-mediated NF-kappaB signaling by cytomegalovirus-encoded deubiquitinase and inactive homolog of cellular ribonucleotide reductase large subunit. PLoS Pathog 13:e1006423. https://doi.org/10.1371/journal.ppat.1006423.

33. Green S, Issemann I, Sheer E. 1988. A versatile in vivo and in vitro eukaryotic expression vector for protein engineering. Nucleic Acids Res 16:369. https://doi.org/10.1093/nar/16.1.369.

34. Lafemina RL, Pizzorno MC, Mosca JD, Hayward GS. 1989. Expression of the acidic nuclear immediate-early protein (IE1) of human cytomegalovirus in stable cell lines and its preferential association with metaphase chromosomes. Virology 172:584–600. https://doi.org/10.1016/0042-6822(89)90201-8.

35. Lee JM, Kang HJ, Lee HR, Choi CY, Jang WJ, Ahn JH. 2003. PIAS1 enhances SUMO-1 modification and the transactivation activity of the major immediate-early IE2 protein of human cytomegalovirus. FEBS Lett 555:322–328. https://doi.org/10.1016/s0014-5793(03)01268-7.